

# Detecting Early Galaxies Through Their 21-cm Signature

Smadar Naoz<sup>†</sup> and Rennan Barkana<sup>†</sup>

<sup>†</sup> *School of Physics and Astronomy, Sackler Faculty of Exact Sciences, Tel Aviv University, Tel Aviv 69978, ISRAEL*  
(February 6, 2020)

New observations over the next few years of the emission of distant objects will help unfold the chapter in cosmic history around the era of the first galaxies. These observations will use the neutral hydrogen emission or absorption at a wavelength of 21 cm as a detector of the hydrogen abundance. We predict the signature on the 21-cm signal of the early generations of galaxies. We calculate the 21-cm power spectrum including two physical effects that were neglected in previous calculations. The first is the redistribution of the UV photons from the first galaxies due to their scattering off of the neutral hydrogen, which results in an enhancement of the 21-cm signal. The second is the presence of an ionized hydrogen bubble near each source, which produces a cutoff at observable scales. We show that the resulting clear signature in the 21-cm power spectrum can be used to detect and study the population of galaxies that formed just 200 million years after the Big Bang.

PACS numbers: 98.80.-k, 98.62.Ai, 98.70.Vc, 95.30.Jx

*Introduction* An important milestone in the evolution of the Universe is the appearance of the first luminous objects, which marks the end of the “Dark Ages” and begins the era of heating and ionization of the intergalactic medium (IGM), referred to as cosmic reionization. A promising probe of the cosmic gas up to the end of reionization is the hyperfine spin-flip transition of neutral hydrogen (H I) at a wavelength of 21 cm. Observations of the redshifted 21-cm power spectrum as a function of wavelength and angular position can provide a three-dimensional map of the distribution of H I [1,2].

The 21-cm line of the hydrogen atom results from the transition between the triplet and singlet hyperfine levels of the ground state. Quantitative calculations of 21-cm absorption begin with the spin temperature  $T_s$ , defined through the ratio between the number densities of hydrogen atoms,  $n_1/n_0 = 3 \exp(-T_\star/T_s)$ , where subscripts 1 and 0 correspond to the excited and ground state levels of the 21-cm transition and  $T_\star = 0.0682$  K corresponds to the energy difference between the levels. The 21-cm spin temperature is on the one hand radiatively coupled to the cosmic microwave background (CMB) temperature  $T_\gamma$ , and on the other hand coupled to the kinetic gas temperature  $T_k$  through collisions [3] or the absorption of Ly $\alpha$  photons, as discussed below. For the concordance set of cosmological parameters [4], the mean brightness temperature on the sky at redshift  $z$  (relative to the CMB itself) is  $\bar{T}_b = 28 \text{ mK} \sqrt{(1+z)/10} [(T_s - T_\gamma)/T_s] \bar{x}_{\text{HI}}$  [2] where  $\bar{x}_{\text{HI}}$  is the mean neutral fraction of hydrogen.

After cosmic recombination, down to  $z \sim 200$  the remaining free electrons kept  $T_k$  close to  $T_\gamma$ . Thus, the 21-cm signal relative to the CMB vanishes at these redshifts. Afterward, the gas cooled adiabatically and atomic collisions kept the spin temperature  $T_s$  coupled to  $T_k$ , both of them lower than  $T_\gamma$ , thus creating a 21-cm signal in absorption. As the universe continued to expand and rarefy the gas, the radiative coupling between  $T_\gamma$  and  $T_s$  started to dominate again, and the 21-cm signal faded. Starting at  $z \sim 66$  [5], the UV photons from the first

galaxies emitted between the Ly $\alpha$  and Lyman limit wavelengths propagated freely in the IGM. They redshifted or scattered into the Ly $\alpha$  resonance, thus coupling  $T_s$  to  $T_k$  through the Wouthuysen-Field (WF) effect whereby atoms re-emitting Ly $\alpha$  photons can de-excite into either of the hyperfine states [6,7].

Fluctuations in the Ly $\alpha$  radiation emitted by the first galaxies led to fluctuations in the 21-cm signal [8], until the WF effect saturated (i.e., finished dropping  $T_s$  to  $T_k$ ). In particular, the biased fluctuations in the number density of galaxies, combined with Poisson fluctuations in the number of galaxies and the  $1/r^2$  dependence of the flux, caused large fluctuations in the Ly $\alpha$  background. This Ly $\alpha$  background is composed of two parts, the photons that directly redshift into the Ly $\alpha$  resonance, and those produced during the atomic cascade from higher Lyman series photons (Ly $\gamma$  and above). About 30% of the total number of photons emitted from the first stars between Ly $\alpha$  and the Lyman limit convert to Ly $\alpha$ , assuming a typical spectrum [9,10]. The 21-cm power spectrum that arises from the fluctuations in the Ly $\alpha$  background can then be used to probe the first sources of light and their effect on the IGM [2,8–11,13,14].

In this *Letter* we focus on two new effects that dramatically influence the Ly $\alpha$  flux fluctuations and therefore the 21-cm power spectrum. The first effect is the diffusion of photons through the H I. Since the optical depth of Ly $\alpha$  is around a million, photons scattered on the surrounding gas cause each source to appear as a halo in the sky rather than a point source [15]. In the absence of scattering a photon will redshift to Ly $\alpha$  at some distance from the source, but in the presence of scattering the emitted photons scatter back and forth and thus reach Ly $\alpha$  much closer to the source [16,17]. Thus, the Ly $\alpha$  flux that a random point in the universe observes is dominated by nearby sources. As a result, the fluctuations in the Ly $\alpha$  flux are larger and enhance the 21-cm power spectrum. The second effect is caused by the presence of ionized hydrogen (H II) around each source [18]. In

this region photons can redshift below the Ly $\alpha$  resonance without encountering H I, and thus not participate in the WF effect. Thus, a given atom receives no Ly $\alpha$  photons from sources closer than the size of a typical H II bubble. Since galaxy number fluctuations below this scale do not contribute to Ly $\alpha$  fluctuations, we expect a cutoff in the 21-cm power spectrum around this scale.

Our calculations are made in a  $\Lambda$ CDM universe matching observations [4], with a power spectrum normalization  $\sigma_8 = 0.826$ , Hubble constant  $H_0 = 68.7 \text{ km s}^{-1} \text{ Mpc}^{-1}$ , and density parameters  $\Omega_m = 0.299$ ,  $\Omega_\Lambda = 0.701$ , and  $\Omega_b = 0.0478$  for matter, cosmological constant, and baryons, respectively.

*Lyman series scattering* We assume a uniform neutral IGM that exhibits pure Hubble expansion around a steady point source [15]. The surrounding IGM, mainly H I, is optically thick to the UV radiation that the source emits. We use a Monte-Carlo method for the scattering [15], for photons of various initial frequencies between Ly $\alpha$  and the Lyman limit. The scattering redistributes the distances at which the photons transform to Ly $\alpha$ , affecting strongly the photons originally emitted between Ly $\alpha$  and Ly $\beta$ . Due to flux conservation, the enhancement of the flux at small scales (by up to a factor of 4 compared to the optically thin case) is balanced by a steep drop at the large scales (where  $\nu \rightarrow \text{Ly}\beta$ ). Ly $\alpha$  photons produced via cascading from photons emitted above Ly $\gamma$  are much less affected. We account for several features that substantially affect the redistribution of photons compared to previous calculations that gave a divergent  $r^{-1/3}$  enhancement near the source [16,17]. First, we explicitly include the H II region around each source, which results in enhanced Ly $\alpha$  scattering just outside the H II region; the enhancement has a shallower rise to a peak value and then drops to zero right near the H II region, because of the loss of photons that are scattered back into the H II region. Second, each hydrogen atom receives Ly $\alpha$  photons from sources with an effective spectrum that drops sharply at frequencies approaching Ly $\beta$ ; photons at such frequencies are emitted by time-retarded sources that formed in a universe with fewer galaxies, effectively reducing the emission rate (see below). We find that scattering strongly enhances this drop in the spectrum. Finally, we also account for the variation of the Hubble constant with redshift, which substantially affects the photons emitted just below Ly $\beta$ .

*21cm Fluctuations* In general, fluctuations in  $T_b$  can be sourced by fluctuations in the gas density, temperature, neutral fraction, radial velocity gradient, and Ly $\alpha$  flux from galaxies. To linear order, perturbing the equation of the brightness temperature, we have  $\delta T_b = \beta_b \delta_b + \beta_T \delta_T + \delta_x + \beta_\alpha \delta_\alpha - \delta_{d_r v_r}$ , where each  $\delta_i$  describes the fractional perturbation on the quantity  $i$  [11,19];  $b$  denotes the baryon density,  $T$  the gas temperature,  $x$  the neutral fraction,  $\alpha$  the Ly $\alpha$  coefficient  $x_\alpha$  (which is simply the Ly $\alpha$  flux measured in

units so that Ly $\alpha$  flux fluctuations give the largest 21-cm fluctuations when  $x_\alpha = 1$ ), and  $d_r v_r$  the line of site velocity gradient (which creates an apparent density fluctuation [12,11]). The associated time-dependent  $\beta_i$  coefficients are  $\beta_b = 1 + [x_c/\tilde{x}_{\text{tot}}]$ ,  $\beta_\alpha = x_\alpha/\tilde{x}_{\text{tot}}$ ,  $\beta_T = [T_\gamma/(T_k - T_\gamma)] + [x_c/\tilde{x}_{\text{tot}}] * [d \log \kappa_{1-0}/d \log T_k]$ , where  $\tilde{x}_{\text{tot}} \equiv x_{\text{tot}}(1 + x_{\text{tot}})$  and  $x_c$  and  $\kappa_{1-0}$  describe the collisional 21-cm excitation [3,11,19]. We consider the high redshift regime before significant external heating. Due to Compton scattering of the CMB photons with the remaining free electrons after cosmic recombination, the baryon temperature fluctuation is not proportional to the baryon density fluctuation [20].

A Fourier transform yields the brightness temperature fluctuation in  $\mathbf{k}$ -space (where  $\tilde{\delta}$  denotes the transform of each  $\delta$  quantity) [11]:

$$\tilde{\delta T}_b(\mathbf{k}, t) = \left( \mu^2 r_{[\delta:\delta]} + \beta \right) \tilde{\delta}_b(\mathbf{k}) + \tilde{\delta}_x(\mathbf{k}) + \beta_\alpha \tilde{\delta}_\alpha(\mathbf{k}), \quad (1)$$

where the ratio  $r_{[\delta:\delta]}(k, z) \equiv [(d/dt)\tilde{\delta}_b]/(H\tilde{\delta}_b)$ ,  $\beta(k, z) \equiv \beta_b + r_{[T:\delta]}\beta_T$  in terms of  $r_{[T:\delta]} \equiv \tilde{\delta}_T/\tilde{\delta}_b$ , and  $\mu = \cos \theta_k$  in terms of the angle  $\theta_k$  of the wavevector  $\mathbf{k}$  with respect to the line of sight. Hereafter we neglect the ionization fluctuations, assuming we are considering a time long before reionization, when ionization fluctuations were negligible compared to the other sources of 21-cm fluctuations.

We denote by  $P_{\delta_b}(k)$  and  $P_\alpha(k)$  the power spectra of the fluctuations in baryon density and in the Ly $\alpha$  flux, respectively, and the power spectrum  $P_{\delta_b-\alpha}$  as the Fourier transform of their cross-correlation function [8]. The 21-cm power spectrum can then be written in the form [11]:  $P_{T_b}(\mathbf{k}) = \mu^4 P_{\mu^4}(k) + \mu^2 P_{\mu^2}(k) + P_{\mu^0}(k)$ , where each of the three  $\mu$  coefficients can be separately measured from their different  $\mu$  dependence [11]. This angular separation of power makes it possible to detect separately different physical aspects influencing the 21-cm signal. In terms of our definitions above, the coefficients are

$$P_{\mu^4}(k) = r_{[\delta:\delta]}^2 P_{\delta_b}(k) \quad (2)$$

$$P_{\mu^2}(k) = 2r_{[\delta:\delta]} [\beta P_{\delta_b}(k) + \beta_\alpha P_{\delta_b-\alpha}(k)]$$

$$P_{\mu^0}(k) = \beta^2 P_{\delta_b}(k) + \beta_\alpha^2 P_\alpha(k) + 2\beta\beta_\alpha P_{\delta_b-\alpha}(k).$$

It is possible to probe whether some sources of  $P_\alpha$  are uncorrelated with  $\delta_b$ ; the quantity

$$P_{\text{un}-\delta}(k) \equiv P_{\mu^0} - \frac{1}{4} \frac{P_{\mu^2}^2}{P_{\mu^4}} = \beta_\alpha^2 \left( P_\alpha - \frac{P_{\delta_b-\alpha}^2}{P_{\delta_b}} \right) \quad (3)$$

receives no contribution from any source that is a linear functional of the baryon density distribution [11].

*The Ly $\alpha$  Flux of Galaxies* We summarize here the calculation of the Ly $\alpha$  flux [8]. The intensity of Ly $\alpha$  photons observed at a given redshift is due to photons that were originally emitted between the rest-frame wavelengths of Ly $\alpha$  and the Lyman limit. Photons that were

emitted below  $\text{Ly}\beta$  by a source simply redshift until they are seen by an atom at  $z$  at the  $\text{Ly}\alpha$  wavelength. Such photons can only be seen out to a distance corresponding to the redshift  $z_{\text{max}}(2)$ , where  $[1 + z_{\text{max}}(2)]/(1 + z) = (32/27)$ , the ratio of  $\text{Ly}\alpha$  to  $\text{Ly}\beta$  wavelengths. Photons above the  $\text{Ly}\beta$  energy redshift until they reach the nearest atomic level  $n$ . The neutral IGM is opaque even to the higher levels and so the photon is absorbed and re-emitted. During these scatterings, the photon has a  $\sim 60\%$  chance to be downgraded to a  $\text{Ly}\alpha$  photon [9,10] and then keep scattering. To be seen at the  $\text{Ly}\alpha$  resonance at  $z$ , the photon must have been emitted below a maximal redshift  $z_{\text{max}}(n)$ . The intensity is thus given by:

$$J_\alpha = \frac{(1+z)^2}{4\pi} \times \sum_{n=2}^{n_{\text{max}}} f_{\text{recyc}}(n) \int_{z_{\text{HII}}}^{z_{\text{max}}(n)} \frac{cdz'}{H(z')} \epsilon(\nu'_n, z') f_{\text{scat}}(n, r), \quad (4)$$

where absorption at level  $n$  at redshift  $z$  corresponds to an emitted frequency  $\nu'_n$  at  $z'$ , and  $\epsilon$  is the photon emissivity [8]. We have included the factor  $f_{\text{recyc}}$  [9,10] which is the fraction of photons absorbed at level  $n$  that are eventually recycled into  $\text{Ly}\alpha$  photons in their subsequent cascade. The new correction factor  $f_{\text{scat}}$  is the overall factor by which the  $\text{Ly}\alpha$  flux is changed due to scattering of photons that are emitted with frequencies between levels  $n$  and  $n+1$  from sources at a comoving distance  $r$  from the final destination at redshift  $z$  (where  $r$  is a function of  $z$  and  $z'$ ). Also new to calculations of the 21-cm power spectrum is the lower limit of the integral ( $z_{\text{HII}}$ ), which accounts for the H II region.

*The 21-cm power spectrum* As mentioned above, there are two separate sources of fluctuations in the  $\text{Ly}\alpha$  flux [8]. The first is density inhomogeneities. Since gravitational instability proceeds faster in overdense regions, the biased distribution of rare galactic halos fluctuates much more than the global dark matter density [21,22]. When the number of sources seen by each atom is relatively small, Poisson fluctuations provide a second source of fluctuations, statistically independent of the first source to linear order. Unlike typical Poisson noise, these fluctuations are correlated between gas elements at different places, since two nearby elements see many of the same sources, though at different distances [8]. Note that although each hydrogen atom receives some  $\text{Ly}\alpha$  flux from sources as far away as 300 comoving Mpc, the fluctuations in flux are actually relatively large because a significant portion of the flux comes from nearby sources.

Due to the geometrical dependence of the flux, the perturbation in the  $\text{Ly}\alpha$  flux due to biased density fluctuations is a linear functional of the underlying density fluctuation field, i.e., the resulting contribution to  $\tilde{\delta}_\alpha(\mathbf{k})$  is related to the Fourier transform of the total density perturbation  $\tilde{\delta}_{\text{tot}}(\mathbf{k})$  by multiplication by an effective window function  $\tilde{W}(k)$  [8]. The total density perturbation

is defined as the mass-weighted mean of the dark matter and baryon perturbations; we also define  $r_{[\delta:\delta_b]} = \tilde{\delta}_{\text{tot}}/\tilde{\delta}_b$ . Under the conditions considered in this paper, the three observable power spectra (eq. 2) can be used to study separately the two sources of  $\text{Ly}\alpha$  fluctuations. In particular, the quantity

$$P_{\text{flux}-\delta}(k) \equiv P_{\mu^2} - \frac{2\beta}{r_{[\delta:\delta]}} P_{\mu^4} = 2r_{[\delta:\delta]} \beta_\alpha r_{[\delta:\delta_b]} \tilde{W}(k) P_{\delta_b}(k) \quad (5)$$

is proportional to the biased-density contribution to  $P_\alpha$ , while  $P_{\text{un}-\delta}(k)$  equals the Poisson contribution to  $P_\alpha$  except for a factor of  $\beta_\alpha^2$ .

*Observable signature* The coupling of the spin temperature to the kinetic temperature through the WF effect requires a relatively low cosmic  $\text{Ly}\alpha$  background, and is expected to occur well before the end of cosmic reionization [2]. We illustrate our results assuming that the  $\text{Ly}\alpha$  coupling transition achieves  $x_\alpha = 1$  at  $z = 20$ ; this requirement determines the star formation efficiency. We assume that galaxies form within all dark matter halos above some minimum mass (or, equivalently, a minimum circular velocity  $V_c = \sqrt{GM/R}$  in terms of the virial radius  $R$ ). We consider a wide range of possible values: galaxies that form through molecular hydrogen cooling ( $V_c = 4.5$  km/s), atomic cooling ( $V_c = 16.5$  km/s), or a minimum mass ten times larger ( $V_c = 35.5$  km/s) due to feedback effects in low-mass halos. We consider a single H II region size (calculated as having the flux-weighted mean volume). This is a reasonable assumption since galaxies at these redshifts are rare and almost all lie in halos close to the minimum halo mass. The H II region size is affected by the fraction  $f_{\text{esc}}$  of stellar ionizing photons that escape into the IGM, and by the stellar population. We consider two extremes, a stellar initial mass function as observed locally (Pop II) or that expected for the very first stars (Pop III; 100 solar mass, zero-metallicity stars).

Each power spectrum contribution ( $P_{\text{flux}-\delta}$  and  $P_{\text{un}-\delta}$ ) starts small on large scales and rises with  $k$ , forming a peak before dropping (and then oscillating) on the scale of the H II region (Figure 1). We summarize the main features of the two power spectra through the peak positions ( $k_{\text{peak}}^{\text{flux}-\delta}$  and  $k_{\text{peak}}^{\text{un}-\delta}$ ) and heights ( $T_{\text{peak}}^{\text{flux}-\delta}$  and  $T_{\text{peak}}^{\text{un}-\delta}$ ). Now, since the flux term would have a peak even without the H II region cutoff [8], the characteristics of its peak are fairly insensitive to the H II region size; thus, we also consider the position of its cutoff, specifically the lowest  $k$  value (above  $k_{\text{peak}}^{\text{flux}-\delta}$ ) where the power spectrum drops to 1 mK:  $k_{1\text{mK}}^{\text{flux}-\delta}$ . Both  $k_{\text{peak}}^{\text{un}-\delta}$  and  $k_{1\text{mK}}^{\text{flux}-\delta}$  essentially measure the size  $R_{\text{HII}}$  of the H II region (Figure 2); in particular, the product  $k_{\text{peak}}^{\text{un}-\delta} * R_{\text{HII}} \approx 0.6$  and  $k_{1\text{mK}}^{\text{flux}-\delta} * R_{\text{HII}} \approx 1.6$ , each to within a factor of 1.5 over a range of three orders of magnitude of  $R_{\text{HII}}$ . On

the other hand, the position and height of the peak of  $P_{\text{flux}-\delta}$  are relatively insensitive to  $R_{\text{HII}}$  and thus observing them would constitute a clear consistency check with the theory. The Poisson peak height  $T_{\text{peak}}^{\text{un}-\delta}$  measures the average number density of galaxies and thus depends mainly on the minimum mass of galactic halos. We note that if significant X-ray heating happened to occur simultaneously with the Ly $\alpha$  coupling transition, then similar fluctuations in the X-ray flux from galaxies would generate 21-cm fluctuations that are even somewhat larger [23]; these fluctuations should similarly be enhanced by scattering and should also show a cutoff at the H II bubble scale.

The five quantitative characteristics we have focused on typically occur at relatively large scales (a fraction of a Mpc, or  $\sim 10$  arcseconds at  $z = 20$ ), and correspond to relatively large (but still linear) fluctuations (1–10 mK). Thus, the predictions are theoretically robust, and require observational capabilities only marginally beyond those of the radio arrays being currently constructed. Given current capabilities, this is the most promising method for firmly detecting and studying the properties of some of the earliest galaxies that ever formed.

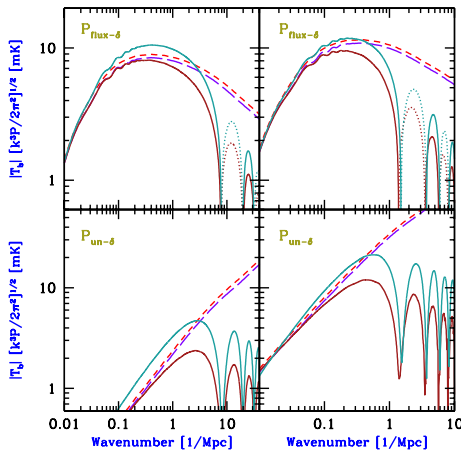


FIG. 1. 21-cm power spectrum  $P$  (shown in terms of the brightness temperature fluctuation at wavenumber  $k$ ) as a function of the comoving wavenumber. We show the two separately-measurable terms that are due to Ly $\alpha$  flux fluctuations arising from biased density fluctuations ( $P_{\text{flux}-\delta}$ ; top panels) or from Poisson fluctuations ( $P_{\text{un}-\delta}$ ; bottom panels). We compare the previous result [8–10] (short-dashed curves) and the result corrected to use the precise density and temperature power spectra [20] (long-dashed curves) to the full calculation with the H II region cutoff (solid curves, with negative portions dotted and shown in absolute value; the higher curve of each pair also includes the redistribution of photons due to scattering). We consider galactic halos with a minimum circular velocity  $V_c = 16.5$  km/s (left panels) or  $V_c = 35.5$  km/s (right panels), assuming Pop II stars with  $f_{\text{esc}} = 0.3$ .

*Acknowledgments* We acknowledge support by Israel Science Foundation grant 629/05 and U.S. - Israel Bina-

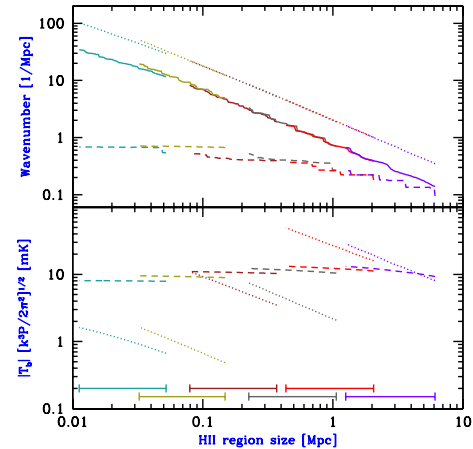


FIG. 2. Main features of 21-cm power spectra from Ly $\alpha$  flux fluctuations as a function of the comoving H II region size. We show (top panel)  $k_{\text{peak}}^{\text{flux}-\delta}$  (dashed curves),  $k_{\text{peak}}^{\text{un}-\delta}$  (solid curves), and  $k_{\text{peak}}^{\text{flux}-\delta}$  (dotted curves), as well as (bottom panel)  $T_{\text{peak}}^{\text{flux}-\delta}$  (dashed curves) and  $T_{\text{peak}}^{\text{un}-\delta}$  (dotted curves). These curves are the result of a sweep of the parameter space, made in six segments each of which varies  $f_{\text{esc}}$  from 1–100% thus covering a range of H II region sizes shown by one of the horizontal bars (bottom panel):  $V_c = 4.5$  km/s with Pop II stars or Pop III stars,  $V_c = 16.5$  km/s with Pop II or III, and  $V_c = 35.5$  km/s with Pop II or III stars, from left to right.

tional Science Foundation grant 2004386.

- 
- [1] C. J. Hogan & M. J. Rees, Mon. Not. R. Astr. Soc. **188**, 791 (1979).
  - [2] P. Madau, A. Meiksin. & M. J. Rees, Astrophys. J. **475**, 429 (1997).
  - [3] A. C. Allison & A. Dalgarno, Astrophys. J. **158**, 423, (1969).
  - [4] D. N., Spergel, et al., Astrophys. J. S. **170**, 377 (2007).
  - [5] S. Naoz, S. Noter & R., Barkana, Mon. Not. R. Astr. Soc. Lett. **373**, L98 (2006).
  - [6] S. A. Wouthuysen, Astrophys. J., **57**, 31 (1952).
  - [7] G. B. Field, Proc. IRE **46**, 240 (1958).
  - [8] R., Barkana, & A., Loeb, Astrophys. J., **626**, 1 (2005b).
  - [9] J. R. Pritchard, S. R. Furlanetto, Mon. Not. R. Astr. Soc. **367**, 1057 (2006).
  - [10] C. M. Hirata Mon. Not. R. Astr. Soc. **367**, 259 (2006).
  - [11] R., Barkana, & A., Loeb, Astrophys. J., **624**, L65 (2005a).
  - [12] S. Bharadwaj & S. S. Ali, Mon. Not. R. Astr. Soc. **356**, 1519 (2004).
  - [13] X. Chen & J. Miralda-Escudé, Astrophys. J. **602**, 1, (2004).
  - [14] L. Chuzhoy, M. A. Alvarez, & P. R. Shapiro, Astrophys. J. Lett. **648** L1, (2006).
  - [15] A. Loeb, & G. B. Rybicki, Astrophys. J. **524**, 527 (1999)

524, 527

- [16] L. Chuzhoy, Z. Zheng, preprint astro-ph/0706.0895
- [17] B. Semelin, F. Combes, S. Baek preprint astro-ph/0707.2483
- [18] R. Barkana, & A. Loeb, Phys. Rep. **349**, 125 (2001).
- [19] S. R. Furlanetto, S. P. Oh, F. H. Briggs, Phys. Rep. **433**, 181 (2006).
- [20] S., Naoz, & R., Barkana, Mon. Not. R. Astr. Soc. **362**, 1047-1053 (2005)
- [21] N. Kaiser, **227**, 1 (1987).
- [22] R., Barkana, & A., Loeb, Astrophys. J., **609**, 474-481 (2004).
- [23] J. R. Pritchard, S. R. Furlanetto, Mon. Not. R. Astr. Soc. **376**, 1680 (2007).